High-throughput Mapping of Leaf Pigment Content from Multispectral Data

Anastasia A. Zolotukhina*, Anastasia V. Guryleva, Sergey S. Ladan, Oksana A. Gusarova, and Alexander S. Machikhin[1]

Acousto-Optic Spectroscopy Lab, Scientific and Technological Center of Unique Instrumentation of the Russian Academy of Sciences, Moscow, Russia

Email: zolotukhina.aa@ntcup.ru (A.A.Z); guryleva.av@ntcup.ru (A.V.G); s.ladan@bk.ru (S.S.L.); gusarova.oa@ntcup.ru (O.A.G.); machikhin@ntcup.ru (A.S.M.)

*Corresponding author

Manuscript received May 30, 2025; revised July 25, 2025; accepted September 29, 2025; published January 19, 2026

***Abstract*—Accurate and timely assessment of the physiological status of plants is crucial for resource optimization and minimizing environmental impact in ecological monitoring and agriculture. This study introduces a novel technique for mapping pigment concentrations in plant leaves using multispectral imaging. The key innovation of the proposed approach is a multispectral camera equipped with reconfigurable spectral filters, enabling application-specific data acquisition. Combined with a data processing protocol, the system achieves high measurement accuracy of leaf pigment content even with limited spectral channels. The technique includes camera calibration, spatiospectral correction, spectral index selection, and nonlinear regression to develop empirical models for estimating chlorophyll concentration. Validation experiments on proximal sensing of lettuce (*Lactuca sativa*) demonstrated that the ratio of Modified Chlorophyll Absorption Ratio Index to Optimized Soil Adjusted Vegetation Index achieved the best performance, with an R^2 of 0.81, an RMSE of 0.3 mg/L, and relative error of less than 20%. Limitations include residual shading and interpolation artifacts, which suggest opportunities for further improvement. The findings highlight high potential of this technique for noninvasive and high-throughput monitoring of plant health in both ecological and agricultural contexts.**

***Keywords*—precision agriculture, remote sensing, pigment content mapping, spectral indices, multispectral imaging**

I. Introduction

Modern ecological monitoring and agriculture increasingly demand accurate and timely assessment of plant physiological status. This allows for optimizing resources such as pesticides and fertilizers while reducing anthropogenic environmental impact. That is why plant condition monitoring tools capable of promptly detecting biotic and abiotic stress are in demand [1, 2]. Traditional vegetation analysis methods, such as visual inspection and biochemical laboratory tests, are limited in both spatial and temporal resolution, highlighting the necessity for new high-throughput approaches [3].

A promising direction in developing plant monitoring tools involves the simultaneous acquisition and processing of multiple spectral images using multispectral imaging. Without spectral and spatial scanning, these devices can capture the spectral characteristics of crops over large areas in real-time. During the technical implementation of such imaging systems, researchers face several critical tasks: determining the principle of spectral data registration; developing a method for correcting inherent data distortions; and creating a method for converting corrected spectral data into relevant plant parameters.

From a technical standpoint, current trends in imaging technology are miniaturization, performance enhancement, and increased adaptability of sensing systems [4]. However, integrating these features into a single device presents significant challenges. A key innovation of the approach is a single-shot multispectral camera with reconfigurable spectral channels, enabling the system to adapt to specific monitoring tasks [5, 6]. This flexibility significantly enhances the precision and applicability of plant health assessments both in remote and proximal sensing.

Since the proposed data acquisition principle is quite novel, the development of data calibration and correction methodology requires further refinement. In addition, interpreting spectral images remains a key challenge: it is essential to convert the obtained spatiospectral distributions into feature maps that represent the physiological state of vegetation and enable a comprehensive assessment of plant health [7, 8]. This task becomes particularly challenging when the number of spectral channels is limited, which is typical for single-shot devices.

This study introduces a novel methodology for mapping the spatial distribution of pigment concentrations in plant leaves based on multispectral data acquired by the proposed camera and validates it in a proximal sensing experiment.

II. Literature Review

A. Quantitative Estimation of Pigment Concentration

The pigment composition of plants is one of the most comprehensive indicators of their physiological state, due to the central role pigments play at various stages of development [9]. Chlorophyll content in plant leaves is influenced by a complex interaction of factors, including climatic conditions, soil properties, light availability, nutrient accessibility, and the genetic traits of individual organisms. Chlorophyll concentration typically decreases under stress and during plant senescence, while the ratio of chlorophyll *a* to *b* changes in response to abiotic stressors such as light deficiency, water stress, soil contamination, and temperature fluctuations. Therefore, measurements of total chlorophyll, chlorophyll *a* and *b*, as well as their ratio, can provide valuable insights into plant-environment interactions [10]. Given the functional significance of pigments in determining plant physiological status, understanding their temporal dynamics and spatial distribution is of practical importance for effective environmental and agricultural management.

A crucial step following spectral data acquisition is processing and interpreting it to determine the spatial distribution of pigments. A well-established and widely used method for analyzing vegetation reflectance spectra is based on spectral indices, which are empirically related to pigment concentrations in plants. Numerous studies have focused on developing and refining techniques for quantitatively estimating chlorophyll concentrations in plant tissues [11]. Chlorophyll absorption bands are typically located at wavelengths of 428–430 nm, 452–455 nm, 642–644 nm, and 660–663 nm. About 30 vegetation indices have demonstrated effectiveness in this task, including the widely known Normalized Difference Vegetation Index (NDVI; 600–700, 750–850 nm) [12], Simple Ratio (SR; 645, 745 nm) [13], modified Normalized Difference (mND_{705}; 705, 750 nm) [14], Chlorophyll Index Red Edge (CI_{RE}; 710, 670 nm) [15], and Enhanced Vegetation Index (EVI; 450, 600–700, 750–850 nm) [16]. Indices such as RECAI (550, 720, 800 nm) [17] minimize the influence of leaf structure, while RSI (704, 815 nm) is suitable for various crops [18]. Several indices based on wavelengths around 705 nm and 750 nm employ equations designed to minimize the effects of soil reflectance, non-photosynthetic materials, incident light angle, and leaf structure, such as MSR, MCARI, TCARI, OSAVI, and the ratio MCARI/OSAVI [19].

B. Optimal Vegetation Index Selection

Multiple studies have been addressed to modify existing indices [10, 11] and develop new ones [17, 20] for pigment estimation. Consequently, selecting the most appropriate spectral index for assessing the physiological state of crops remains a challenge due to the numerous factors that affect reflectance spectra. Leaf structure, water content, nutrient status, disease presence, pigmentation, phyllotaxis, sun exposure, and phenological stage are just a few of these influencing variables. Each spectral index was initially developed using a specific dataset, which limits its sensitivity to pigment content under changing conditions. Additionally, indices may be specific to particular sensors and spatial scales (e.g., ground-based and satellite), highlighting the importance of choosing the optimal index for each specific application [21]. In the case of hyperspectral systems, Zolotukhina *et al.* [22] proposed selecting the optimal index and empirical model based on determination coefficients and relative error, with pigment content determined by standardized analytical methods. Acoustic-optical filtering allows arbitrary spectral tuning and can reduce the time required to capture all spectral images for computing various indices [23, 24].

C. Multispectral Imagers

There are two main reasons for investigating the feasibility of multispectral approaches in pigment mapping. First, multispectral imagers typically offer outstanding performance for agricultural applications, including compact size and weight, high imaging speed, and transmittance [4, 25, 26]. This study proposes a multispectral snapshot camera based on dividing the optical aperture into different spectral channels and simultaneously acquiring all spectral images with a single sensor [5, 6]. This is a novel principle for diagnostic imaging in agriculture and has several advantages, including the absence of crosstalk typically found in other multispectral imaging systems [26]. Another benefit over mentioned cameras is the ability to relatively easily change channels spectral bands and the spectral range width, which is limited only by the sensor spectral sensitivity. Some camera designs offer similar capabilities, for example, systems with filter wheels which remain relatively bulky and have reduced reliability due to moving parts [27]. Cameras with multiple optical systems and separate sensors also allow filters to be changed; however, they have a limited number of channels and significant parallax [28–30]. Other advantages of our camera include the accurate temporal synchronization of registration and alignment of sensor spectral sensitivity for different channels at the hardware level, which is difficult to achieve in other systems.

The closest analogue of the proposed camera uses a different element for spectral channel separation and therefore cannot be considered fully reconfigurable [31]. The novelty of the proposed system necessitates the development of algorithms to correct inevitably occurring data distortions. These algorithms are generally based on known processing methods that are either suitable for or adapted to the specific device. The algorithm for the proposed multispectral system can be based on previously known methods for correcting spectral and spatial sensitivity non-uniformity, dark current, aberrations, and parallax [4, 22, 32].

The second reason is limited number of spectral bands in multispectral cameras, which makes the selection of the optimal index particularly important. However, this approach has not yet been thoroughly investigated for multispectral cameras with a limited number of channels. T. Boonupara *et al*. [33] suggested a method for determining correlations between a set of indices and pigment concentrations using multispectral data from a 5-band camera. The study identified the Enhanced Vegetation Index (EVI) as the most suitable for monitoring pigment content in lettuce, showing a correlation coefficient of 0.85 with chlorophyll concentration. Furthermore, in these terms, the proposed reconfigurable design provides additional flexibility in solving tasks and enables obtaining more accurate data without significant investments in updating or replacing the device.

D. Proposed Approach

In this study, a versatile approach to pigment concentration mapping is presented and validated in a proximal sensing experiment. To this end, a multispectral camera with interchangeable spectral filters was developed. It allows for optimized data acquisition. When the optimal wavelengths related to proper spectral indices are established, the camera may be tuned to image collection strictly in those bands. Thus, using a single instrument, high-throughput and accurate mapping of leaf pigment content becomes available for multiple crops and environmental conditions.

III. Materials and Methods

A. Biological Samples

The object of the study was cultivated lettuce (*Lactuca sativa*), an annual herbaceous plant characterized by rapid growth and high sensitivity to environmental conditions, which makes it a common model organism in plant physiology research. The overall experimental design included six early-maturing cultivars (45–55 days to harvest

maturity), sown at 20-day intervals under two mineral nutrition regimes, with four replicates per treatment. The use of staggered sowing allowed simultaneous observation of plants at different physiological development stages during each measurement session, significantly enhancing the precision and reliability of the observations.

Standard 24-cell trays were used for planting. Non-pelleted seeds were sown at a density of 5–7 plants per cell into a cotton-mineral substrate placed in mesh pots 50 mm × 50 mm. The nutrient solution fully complemented essential elements (N 131, P 45, K 224, Ca 85, Mg 59, S 21, EC 1.7–1.6, N:K ratio 1:1.7) and a half-strength version, corresponding to the two nutritional treatments. During the experiment, two of six cultivars were excluded from further observations due to delayed initial development, which may indicate a more extended vegetative growth period under artificial conditions than specified by the seed breeder for open-field cultivation. As the comparison between varieties was beyond the scope of this study, this does not compromise the statistical validity of the results.

Nutrient delivery was performed with a frequent sub-irrigation method, which provided better root aeration under the given conditions than a continuous flow system. The solution was supplied to the trays for 25 min, with a 60-minute interval between irrigations. Lighting conditions were constant across all treatments at approximately 10-12 klx, with a photoperiod of 10 h per day.

B. Laboratory Studies

Spectral imaging of the lettuce pots was conducted under stable laboratory conditions in proximity sensing scenario. Each sample was placed on a dark background and illuminated by two halogen light sources positioned at 45° angles from opposite sides to minimize shadowing. A multispectral camera was mounted 1 m above the sample, with the sensor plane aligned parallel to the table surface, ensuring the entire plant was fully captured within the frame of each spectral channel. For radiometric correction, a reference panel was recorded under identical lighting and registration conditions before imaging the samples. The reference panel was made of fluoropolymer and served as a reference object with a reflectance coefficient close to 1 across the entire spectral range of the imager.

A standard method for measuring pigment content involves spectrophotometric analysis of a pigment extract obtained through sample preparation [22]. Plant leaves were weighed to obtain a specific sample mass (170 mg), then homogenized in a mortar. Pigments were extracted using ethanol (25 mL). The optical density of the extract was measured by a spectrophotometer to quantify the total chlorophyll a and b content Chl (in mg/L), based on established empirical relationships [34]:

$$Chl = 6.1 \cdot D_{665} + 20.04 \cdot D_{649}, \quad (1)$$

where D_{665} and D_{649} are the optical densities of the extract at wavelengths of 665 and 649 nm.

C. Hardware

In this study, a multi-aperture spectral camera was employed [5], featuring eight spectral channels covering the 450–800 nm range, evenly spaced central wavelengths at 50 nm intervals, and a bandwidth of 30 nm, with a field of view of 55×70° and a frame rate up to 18 frames per second at a full resolution (Fig. 1). This device's principle of simultaneous spectral data acquisition is the simultaneous acquisition of multiple spectral images by a single imaging sensor using a multi-aperture system and a spectral lens array. The selected spectral range, on the one hand, covers the regions most sensitive to chlorophyll, and on the other hand, corresponds to the standard sensitivity range of available radiation detectors. Eight uniformly distributed wavelengths serve to cover the entire spectral range and enable the calculation of a wide range of spectral indices.

The division of the optical aperture into independent spectral channels offers several advantages. First, integrating the spectral channels into a modular multispectral unit allows their fast replacement. Second, this design eliminates the crosstalk typically found in alternative imagers based on mosaic filters applied directly to the sensor at the pixel level. Additionally, a single imaging sensor removes the necessity to synchronize data streams from multiple detectors, reducing the system's mass and dimensions. As a result, the proposed camera demonstrates enhanced adaptability and operational convenience for both remote and proximal sensing, while providing data of higher reliability and informativeness.

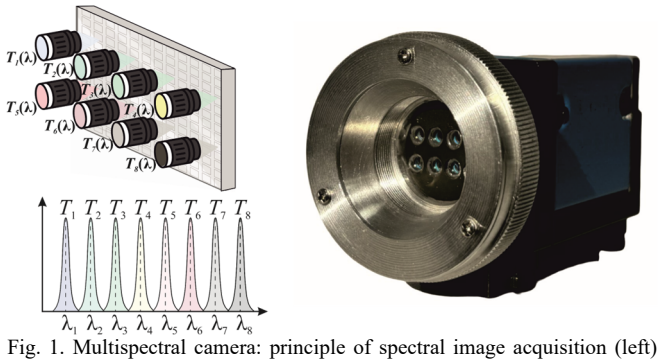

Fig. 1. Multispectral camera: principle of spectral image acquisition (left) and appearance (right). Eight lenses and filters generate spectral images on a single CMOS sensor. The transmission functions of the filters exhibit minimal overlap and have Gaussian profiles.

The objective of spectral imaging is to reconstruct the spatial distribution of the surface spectral reflectance coefficient $\rho(x, y, \lambda)$. However, due to the wide variety of multispectral cameras and their design based on different physical principles, there is no standardized correction procedure. As a result, a calibration algorithm must take into account a significant number of factors that may distort the output data.

D. Camera Calibration

A spectral reflectance coefficient for each pixel $\rho(x, y, \lambda)$ is essential for assessing the condition of plants. However, the output data from a multispectral camera does not directly provide the reflectance coefficient. Instead, it offers a spatial distribution of the object's spectral radiance. This data is further complicated by inevitable distortions caused by the camera's key components: spectral filters, the optical system, and the sensor [32]. Thus, acquired images $I'(x, y, \lambda)$ must undergo calibration and radiometric correction prior to the direct extraction of plant features.

Table 1 outlines the key parameters that need to be considered during calibration, together with relevant variables for mathematical calibration modelling. Table 1 also includes references that detail the impact these parameters have on the data and effective methods for

addressing and eliminating the associated distortions. Proper attention to these calibration parameters, along with their correct application, is vital for achieving reliable and accurate results in plant condition assessment through spectral measurements.

Table 1. Sources of data distortions

Parameters	Variable	Ref.
The dark current noise of the sensor	$I_t(x,y,\lambda)$	[35]
The non-linearity of the sensor response	α, β, γ	[36]
The optical vignetting	$K_v(x,y,\lambda)$	[22]
The non-uniformity of the sensor's spectral sensitivity	$K_s(x,y,\lambda)$	[32]
Optical geometric distortions	$\Delta x_d(x,y,\lambda)$, $\Delta y_d(x,y,\lambda)$	[37]
Geometric distortions due to parallax	$\Delta x_p(\lambda), \Delta y_p(\lambda)$	[32]

The spatiospectral distribution of a raw signal $I'(x,y,\lambda)$ provided by the multispectral camera can be expressed as follows:

$$I'(x,y,\lambda) == \alpha + \beta\left\{K_s(x,y,\lambda)\cdot K_v(x,y,\lambda)\cdot \cdot I\begin{bmatrix} x+\Delta x_p(\lambda)+\Delta x_d(x,y,\lambda), \\ y+\Delta y_p(\lambda)+\Delta y_d(x,y,\lambda), \lambda \end{bmatrix}\right\}^{\gamma} + I_t(x,y,\lambda) \quad (2)$$

At the calibration stage, the variables from Eq. (2) are quantified and subsequently corrected. Fig. 2 illustrates the workflow of this procedure. Correction of these distortions requires prior calibration of the multispectral camera to determine the appropriate correction coefficients. Image acquisition was carried out with the lens cap closed over a range of exposure times to assess dark current noise. To determine the sensor's response nonlinearity [38] and vignetting pattern [36], the output port of the integrating sphere (Labsphere Spectra-FT-2300-W) was imaged across varying brightness levels and exposure durations. Spectral sensitivity was assessed with a tunable monochromatic light source (Solar Laser Systems M266i–IV). Calibration targets, such as a checkerboard pattern and reference markers, were imaged to correct optical distortion and align the images.

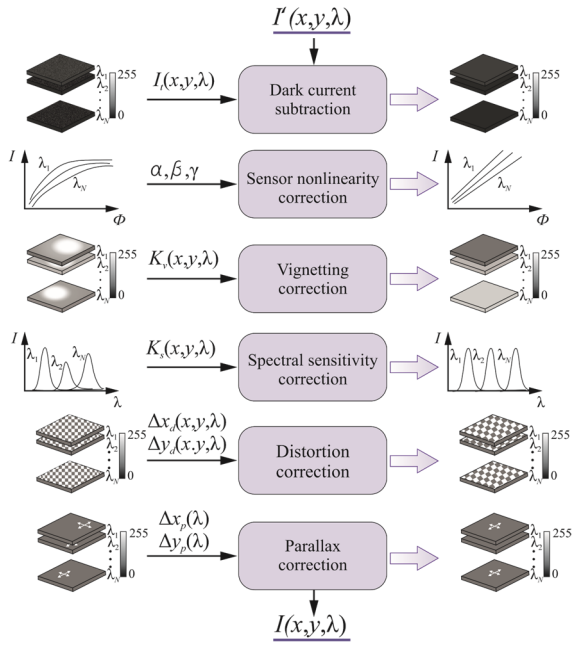

Fig. 2. Calibration pipeline.

After spectral images of the samples and the reference panel were corrected, the spatial distribution of the surface spectral reflectance $\rho(x,y,\lambda)$ was determined using the flat-field method [39]. A binary mask was then generated to isolate only the pixels corresponding to lettuce leaves, based on the ratio of reflectance at 750 nm and 650 nm wavelengths, followed by thresholding (threshold = 1.3). Ten vegetation indices known to be sensitive to chlorophyll content were calculated from the mean reflectance spectrum of all leaf pixels in each sample. To estimate these indices under the limited spectral resolution, Akima spline interpolation was used due to its ability to preserve local variations without distortions [40]. Considering the nonlinear relationship between vegetation indices and pigment concentration reported in [41], nonlinear regression to establish empirical relationships between the index values and chlorophyll content was applied. The optimal model and corresponding vegetation index were selected according to the highest coefficient of determination R^2. The resulting empirical relationship is then applied to each pixel of the optimized vegetation index map to generate the spatial distribution of chlorophyll concentration in plant leaves. Image processing algorithm and statistical analysis was implemented in MATLAB. Data acquisition and processing was performed on a personal computer with CPU Intel Core i5-13420H, Intel UHD Graphics, and RAM 16 Gb.

IV. Results and Discussion

A. Spatiospectral Correction

The multispectral camera was calibrated to obtain distortion correction coefficients. Spectral data from 15 lettuce samples were corrected using the proposed algorithm. Fig. 3 shows examples of raw images and the corrected results as a spatial distribution of the reflectance coefficient $\rho(x,y,\lambda)$.

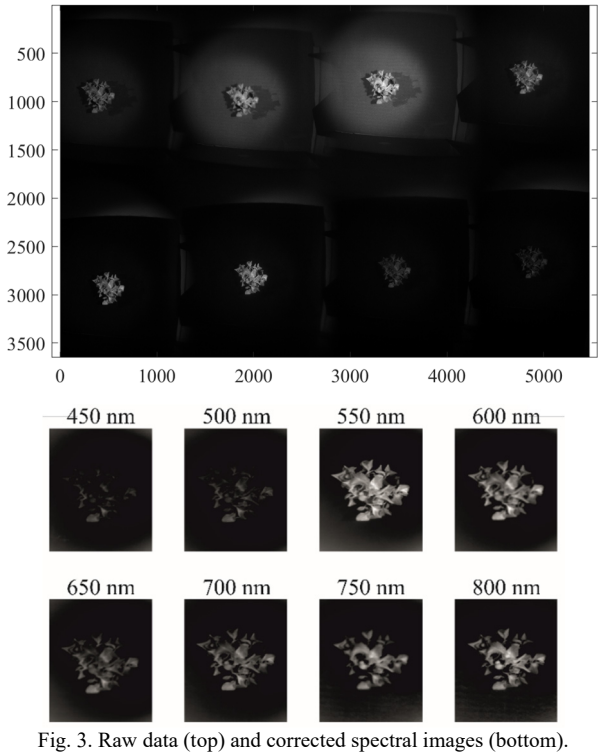

Fig. 3. Raw data (top) and corrected spectral images (bottom).

Next, a mask was generated for each sample to isolate the pixels corresponding to the plant leaves. To calculate vegetation indices further, the reflectance coefficient was averaged over these pixels (Fig. 4).

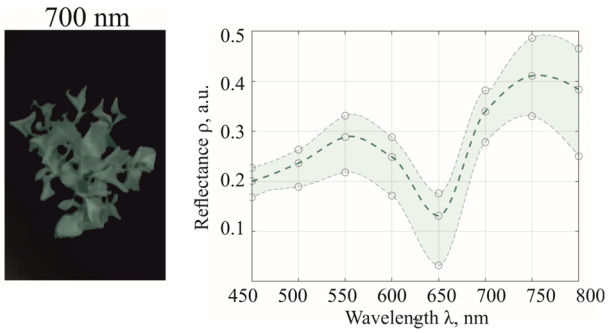

Fig. 4. Example of applying a mask (left) and the mean reflectance spectrum with its variability across the samples, calculated for the highlighted area (right).

B. Mapping Leaf Pigment Content

For each index, an empirical model $y = a \cdot x^b + c$ was determined using the least squares method. The model parameters and the adjustment criterion are presented in Table 2. Table 2 indicates that the MCARI/OSAVI index is the best predictor of chlorophyll concentration among those considered, which can be explained by the index's chlorophyll sensitivity and the stability across various lighting conditions and plant developmental stages [42].

Table 2. Model parameters

VI	Model parameters				
	a	***b***	***c***	R^2	***RMSE***, mg/L
CI_{RE}	-0.6637	-0.4565	0.5306	0.61	0.06
MSR	-0.4134	-0.5887	0.3203	0.62	0.04
MTCI	-0.4343	-0.6187	0.3305	0.60	0.04
MCARI	-0.2661	-0.4327	0.2018	0.55	0.02
MCARI/ OSAVI	**-5.9780**	**-2.0910**	**0.9247**	**0.81**	**0.3**
$NDVI_{705}$	-0.2723	-0.6006	0.2107	0.63	0.03
OSAVI	-0.2636	-0.5927	0.2045	0.62	0.02
RECAI	0.0687	0.7606	-0.1649	0.26	0.07
EVI	-0.0004	4.3420	1.5410	0.02	1.72
RSI	1.4640	0.1235	-0.6014	0.46	0.08

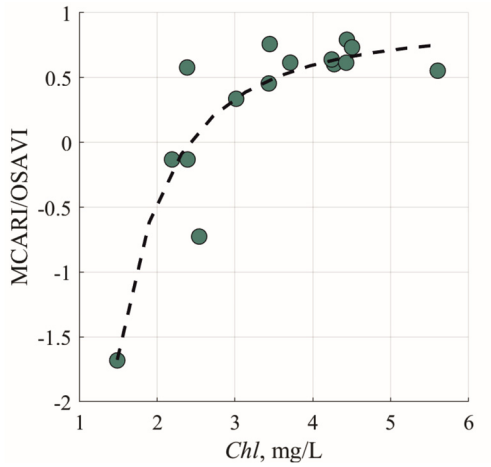

Fig. 5. Empirical model for calculating the chlorophyll content from MCARI/OSAVI index.

Fig. 5 illustrates the model with the highest coefficient of determination, based on the MCARI/OSAVI index, along with the corresponding scatterplot.

The spatial distributions of chlorophyll concentration were obtained by applying the derived model to each pixel of the selected vegetation index map. Some of them are shown in Fig. 6.

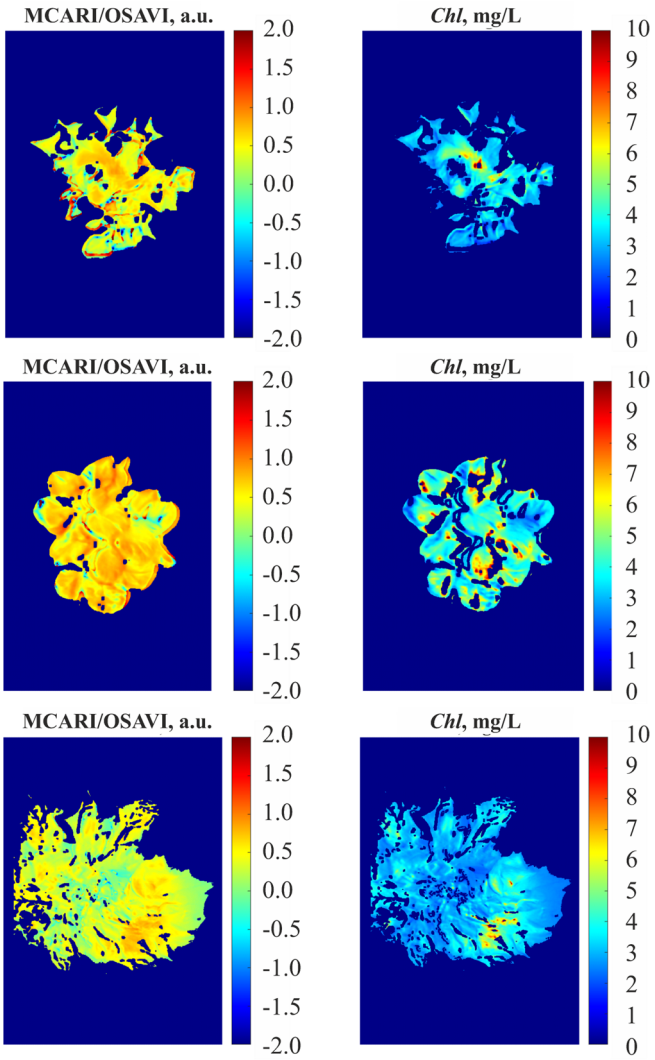

Fig. 6. Maps of total chlorophyll content in lettuce leaves.

C. Error Assessment

The average relative error in pigment content using the derived model is less than 20% and the R^2 is more then 0.81, while other studies report errors as a rule in the range of 5–20% [43, 44] and 0.65–0.95, consequently [20, 45]. The study's results could be significantly improved by selecting spectral channels through hyperspectral imaging and then applying a multispectral approach. Hyperspectral data provide higher spectral resolution, allowing for precise identification of spectral features of plants and detection of channels most sensitive to changes in pigment content. Subsequently, a multispectral camera with optimized channels will yield more accurate and efficient results in monitoring the physiological state of the plants. This approach helps reduce information loss and enhances the accuracy of calculations, providing more reliable data for assessing the condition of crops. Furthermore, the proposed design of the multispectral camera allows for the selection and replacement of spectral channels, offering flexibility and

adaptability for different tasks and crop types.

The data interpolation using Akima splines effectively compensated for the limited spectral channels at low resolution. In our study, the spectral channels were evenly distributed, minimizing distortions typical of interpolation. This method proved suitable as it facilitates the calculation of all necessary vegetation indices despite the limited number of channels.

The limitations affecting the reliability of proposed multispectral approach for pigment mapping can be divided as follow: factors related to the imager, to conditions for data acquisition, to the data processing algorithm, and to the study subject. The primary features associated with the device is the influence of the central wavelength, as well as the shape and width of the spectral band, on the spectral indexes value and model accuracy. While the influence of the central wavelength was considered in other studies, the issues of width and shape are much less frequently taken into account [46].

Lighting conditions of the object also have a significant impact on the results. The pigment concentration maps reveal residual shadow effects from the leaves, indicating some distortions during spectral data acquisition. Despite data correction methods and optimization of image acquisition conditions, shadows and varying leaf inclinations remain significant factors affecting the accuracy of pigment concentration estimation in certain leaf areas. These factors are discussed in previous studies [21]. Improving lighting conditions and applying methods for extracting the diffuse component of reflected radiation may help minimize this effect, enhancing the accuracy of pigment concentration mapping [47].

Since the presented processing algorithm is free from manually performed stages and the methods used are based on well-established and proven techniques, the primary source of uncertainty in the processing algorithm is rather the conversion of spectral data into pigment concentration values. This includes: selection of a set of related spectral indices, method of constructing an empirical model, metrics for assessing the model. An important aspect is also the acquisition of validating data, i.e., the method and accuracy of standard laboratory analyses.

The most significant uncertainty in the results can be introduced by plant morphology. The effectiveness of the model can vary significantly depending on the crop and leaf shape, as well as the growth stage of the plant species [48]. This issue can be addressed through the proposed methodology for determining the empirical model for each new crop.

Selecting a distortion-resistant index becomes particularly crucial in field conditions. Proposed methodology holds promise for overcoming this challenge. Calibration procedures should be adjusted to suit the particularities of field data collection. Additional research is required to fine-tune calibration stages, leveraging established methodologies [49, 50]. Moving from lab-based studies to field deployment, combined with integrating artificial intelligence into devices, and enhancing specialization for specific tasks is a natural for agrophotonics development. The foundational studies on vegetation indices from the past decades [51, 52] have paved the way for today's advanced robotic and automated diagnostic systems, which are used in diverse field applications [53, 54].

V. Conclusion

Multispectral imaging is one of the most promising technologies for plant diagnostics in agriculture. The authors aimed to fill the research gap regarding the feasibility of a reconfigurable multispectral camera for mapping plant pigments under proximal conditions. A novel snap-shot multispectral camera based on the principle of optical aperture division and simultaneous spectral images acquisition by a single sensor was introduced. This camera features several advantages, including the absence of channels crosstalk and the ability to easily adjust spectral bands and spectral range width. Additionally, a data correction algorithm was developed to address inevitable distortions in the acquired data. This algorithm is based on established processing methods adapted specifically for the suggested imager. An approach to non-contact assessing the total chlorophyll concentration in plants using multispectral imaging and determining the spatial distribution of the optimal vegetation index was proposed. The effectiveness of a multispectral camera with 8 channels evenly distributed in the range of 450–800 nm for monitoring plant health was demonstrated under proximal conditions. The study results showed that the proper correction models and the optimization of imaging conditions allow the determination of the spatial distribution of pigment concentrations in leaves. The proposed method is characterized by an average relative error of less than 20% and a root mean square error of 0.3 mg/L, and it offers valuable opportunities for ecological and agricultural applications, such as precision agriculture, greenhouse management, and water stress monitoring, by improving the accuracy of plant physiological status assessment.

The proposed camera, along with the data acquisition and processing method, offers several advantages over existing systems, including adaptable design for various tasks, data reliability, compact size, weight, as well as a low cost and performance comparable to hyperspectral cameras. These benefits make it a promising tool for versatile pigment concentration mapping, applicable to both proximal sensing in laboratory conditions and remote sensing with unmanned aerial vehicles. However, during the study, residual shadow effects from the leaves were observed, which require further improvement of the proposed methodology. Further calibration of multispectral imager, analysis of the influence of individual processing steps on method robustness, and the development of advanced correction techniques will enhance the accuracy of pigment concentration mapping and ensure more effective crop health monitoring. An important next step will be testing the system under field conditions to validate its robustness and applicability in real-world agricultural and ecological scenarios, as well as integration with machine learning, and adaptation to other crops.

Conflict of Interest

The authors declare no conflict of interest.

Author Contributions

Conceptualization, ASM; methodology, AAZ, AVG and

ASM; data curation, OAG and SSL; software, AAZ; validation, OAG and SSL; investigation, AVG, AAZ and SSL; writing—original draft preparation, ASM and AAZ; writing—review and editing, AVG and SSL; visualization, AAZ; supervision, project administration and funding acquisition, ASM. All authors have read and agreed to the published version of the manuscript.

FUNDING

This study is supported by Russian Science Foundation (project 25-16-00121).

ACKNOWLEDGMENT

This work was performed using the equipment of the Center for Collective Use of STC UI RAS [http:// https://ckp.ntcup.ru/en/].

REFERENCES

[1] D. W. Girmaw, A. O. Salau, B. S. Mamo, and T. L. Molla, "A novel deep learning model for cabbage leaf disease detection and classification," *Discover Applied Sciences*, vol. 6, no. 10, pp. 1–20, Oct. 2024. doi: 10.1007/s42452-024-06233-1

[2] B. M. Dodamani, R. Anoop, and D. R. Mahajan, "Agricultural drought modeling using remote sensing," *International Journal of Environmental Science and Development*, vol. 6, no. 4, pp. 326–331, 2015. doi: 10.7763/IJESD.2015.V6.612

[3] H. Zhang, Y. Ge, X. Xie, A. Atefi, N. K. Wijewardane, and S. Thapa, "High throughput analysis of leaf chlorophyll content in sorghum using RGB, hyperspectral, and fluorescence imaging and sensor fusion," *Plant Methods*, vol. 18, no. 1, pp. 1–17, Dec. 2022. doi: 10.1186/s13007-022-00892-0

[4] M. Barjaktarovic, M. Santoni, and L. Bruzzone, "Design and verification of a low-cost multispectral camera for precision agriculture application," *IEEE Journal of Selected Topics in Applied Earth Observations and Remote Sensing*, vol. 17, pp. 6945–6957, 2024. doi: 10.1109/JSTARS.2024.3377104

[5] V. I. Batshev, A. V. Krioukov, A. S. Machikhin, and A. A. Zolotukhina, "Multispectral video camera optical system," *Journal of Optical Technology*, vol. 90, no. 11, p. 706, Nov. 2024. doi: 10.1364/JOT.90.000706

[6] S. A. Mathews, "Design and fabrication of a low-cost, multispectral imaging system," *Applied Optics*, vol. 47, no. 28, pp. F71–F76, Oct. 2008. doi: 10.1364/AO.47.000F71

[7] A. O. Salau and S. Jain, "Feature extraction: A survey of the types, techniques, applications," in *Proc. 2019 International Conference on Signal Processing and Communication (ICSC)*, Mar. 2019, pp. 158–164. doi: 10.1109/ICSC45622.2019.8938371

[8] Y. F. Li, X. G. Xu, W. B. Wu *et al.*, "Hyperspectral estimation of chlorophyll content in grapevine based on feature selection and GA-BP," Scientific Reports, vol. 15, no. 1, pp. 1–13, Dec. 2025. doi: 10.1038/s41598-024-84977-x

[9] A. A. Clemente, G. M. Maciel, A. C. S. Siquieroli *et al.*, "High-throughput phenotyping to detect anthocyanins, chlorophylls, and carotenoids in red lettuce germplasm," *International Journal of Applied Earth Observation and Geoinformation*, vol. 103, 102533, Dec. 2021. doi: 10.1016/j.jag.2021.102533

[10] G. A. Blackburn, "Hyperspectral remote sensing of plant pigments," *Journal of Experimental Botany*, vol. 58, no. 4, pp. 855–867, Mar. 2007. doi: 10.1093/jxb/erl123

[11] M. F. Taha *et al.*, "High-throughput analysis of leaf chlorophyll content in aquaponically grown lettuce using hyperspectral reflectance and RGB images," *Plants*, vol. 13, no. 3, p. 392, Jan. 2024. doi: 10.3390/plants13030392

[12] H. K. Lichtenthaler, M. Lang, M. Sowinska, F. Heisel, and J. A. Miehé, "Detection of vegetation stress via a new high resolution fluorescence imaging system," *Journal of Plant Physiology*, vol. 148, no. 5, pp. 599–612, Jan. 1996. doi: 10.1016/S0176-1617(96)80081-2

[13] G. S. Birth and G. R. McVey, "Measuring the color of growing turf with a reflectance spectrophotometer," *Agronomy Journal*, vol. 60, no. 6, pp. 640–643, Nov. 1968. doi: 10.2134/agronj1968.00021962006000060016x

[14] D. A. Sims and J. A. Gamon, "Relationships between leaf pigment content and spectral reflectance across a wide range of species, leaf structures and developmental stages," *Remote Sensing of Environment*, vol. 81, no. 2–3, pp. 337–354, 2002. doi: 10.1016/S0034-4257(02)00010-X

[15] C. S. T. Daughtry, C. L. Walthall, M. S. Kim, E. B. De Colstoun, and J. E. McMurtrey, "Estimating corn leaf chlorophyll concentration from leaf and canopy reflectance," *Remote Sensing of Environment*, vol. 74, no. 2, pp. 229–239, Nov. 2000. doi: 10.1016/S0034-4257(00)00113-9

[16] H. Q. Liu and A. Huete, "A feedback based modification of the NDVI to minimize canopy background and atmospheric noise," *IEEE Transactions on Geoscience and Remote Sensing*, vol. 33, no. 2, pp. 457–465, Mar. 1995. doi: 10.1109/36.377946

[17] B. Cui, Q. J. Zhao, W. j. Huang *et al.*, "A new integrated vegetation index for the estimation of winter wheat leaf chlorophyll content," *Remote Sensing*, vol. 11, no. 8, 2019. doi: 10.3390/rs11080974

[18] Y. Inoue *et al.*, "Simple and robust methods for remote sensing of canopy chlorophyll content: a comparative analysis of hyperspectral data for different types of vegetation," *Plant, Cell & Environment*, vol. 39, no. 12, pp. 2609–2623, 2016. doi: 10.1111/pce.12815

[19] D. Haboudane, J. R. Miller, N. Tremblay, P. J. Zarco-Tejada, and L. Dextraze, "Integrated narrow-band vegetation indices for prediction of crop chlorophyll content for application to precision agriculture," *Remote Sensing of Environment*, vol. 81, no. 2–3, pp. 416–426, 2002. doi: 10.1016/S0034-4257(02)00018-4

[20] J. C. O. Koh, B. P. Banerjee, G. Spangenberg, and S. Kant, "Automated hyperspectral vegetation index derivation using a hyperparameter optimisation framework for high-throughput plant phenotyping," *New Phytologist*, vol. 233, no. 6, pp. 2659–2670, Mar. 2022. doi: 10.1111/nph.17947

[21] H. Zhang, L. Wang, X. Jin, L. Bian, and Y. Ge, "High-throughput phenotyping of plant leaf morphological, physiological, and biochemical traits on multiple scales using optical sensing," *The Crop Journal*, vol. 11, no. 5, pp. 1303–1318, Oct. 2023. doi: 10.1016/j.cj.2023.04.014

[22] A. Zolotukhina, A. Machikhin, A. Guryleva, V. Gresis, and V. Tedeeva, "Extraction of chlorophyll concentration maps from AOTF hyperspectral imagery," *Frontiers in Environmental Science*, vol. 11, Apr. 2023. doi: 10.3389/fenvs.2023.1152450

[23] O. I. Korablev, D. A. Belyaev, Y. S. Dobrolenskiy *et al.*, "Acousto-optic tunable filter spectrometers in space missions," *Applied Optics*, vol. 57, no. 10, Apr. 2018. doi: 10.1364/AO.57.00C103

[24] V. Pozhar *et al.*, "Hyper-spectrometer based on an acousto-optic tuneable filters for UAVS," *Light & Engineering*, pp. 99–104, Jun. 2019. doi: 10.33383/2018-029

[25] D. Mengu, A. Tabassum, M. Jarrahi, and A. Ozcan, "Snapshot multispectral imaging using a diffractive optical network," *Light: Science & Applications*, vol. 12, no. 1, pp. 1–20, Dec. 2023. doi: 10.1038/s41377-023-01135-0

[26] C. Williams, G. S. D. Gordon, T. D. Wilkinson, and S. E. Bohndiek, "Grayscale-to-color: Scalable fabrication of custom multispectral filter arrays," *ACS Photonics*, vol. 6, no. 12, pp. 3132–3141, Dec. 2019. doi: 10.1021/acsphotonics.9b01196

[27] F. Akkoyun, "Inexpensive multispectral imaging device," *Instrumentation Science & Technology*, vol. 50, no. 5, pp. 543–559, 2022. doi: 10.1080/10739149.2022.2047061

[28] T. Sakamoto, D. Ogawa, S. Hiura, and N. Iwasaki, "Alternative procedure to improve the positioning accuracy of orthomosaic images acquired with Agisoft Metashape and DJI P4 Multispectral for crop growth observation," *Photogrammetric Engineering & Remote Sensing*, vol. 88, no. 5, pp. 323–332, May 2022. doi: 10.14358/PERS.21-00064R2

[29] P. Carril, I. Colzi, R. Salvini *et al.*, "Multispectral, thermographic and spectroradiometric analyses unravel bio-stimulatory effects of wood distillate in field-grown chickpea (*Cicer arietinum* L.)," *Remote Sensing*, vol. 16, no. 14, p. 2524, Jul. 2024. doi: 10.3390/rs16142524

[30] A. Saccuti, F. Graziosi, and D. Lodi Rizzini, "A dataset for vineyard disease detection via multispectral imaging," *Data in Brief*, vol. 61, Aug. 2025. doi: 10.1016/j.dib.2025.111712

[31] Y. Liu *et al.*, "A novel hybrid-DCNN-based framework for enhanced rice aboveground biomass estimation under limited samples," *IEEE Transactions on Geoscience and Remote Sensing*, vol. 63, 2025. doi: 10.1109/TGRS.2025.3544343

[32] A. A. Zolotukhina *et al.*, "Algorithm for the spatial-spectral correction of data captured by a multispectral camera," *Bulletin of the Russian Academy of Sciences: Physics*, vol. 89, no. 4, pp. 590–594, Apr. 2025. doi: 10.1134/S1062873825710852

[33] T. Boonupara, P. Udomkun, and P. Kajitvichyanukul, "Quantitative analysis of atrazine impact on UAV-derived multispectral indices and correlated plant pigment alterations: A heatmap approach," *Agronomy*, vol. 14, no. 4, Apr. 2024. doi: 10.3390/agronomy14040814

[34] J. F. G. M. Wintermans and A. De Mots, "Spectrophotometric characteristics of chlorophylls a and b and their phenophytins in ethanol," *Biochimica et Biophysica Acta (BBA) - Biophysics including Photosynthesis*, vol. 109, no. 2, pp. 448–453, Nov. 1965. doi: 10.1016/0926-6585(65)90170-6

[35] W. C. Porter, B. Kopp, J. C. Dunlap, R. Widenhorn, and E. Bodegom, "Dark current measurements in a CMOS imager," in *Proc. SPIE*, Feb. 2008, vol. 6816, pp. 98–105. doi: 10.1117/12.769079

[36] H. Cao, X. Gu, X. Wei, T. Yu, and H. Zhang, "Lookup table approach for radiometric calibration of miniaturized multispectral camera mounted on an unmanned aerial vehicle," *Remote Sensing*, vol. 12, no. 24, Dec. 2020. doi: 10.3390/rs12244012

[37] Z. Zhang, "A flexible new technique for camera calibration," *IEEE Transactions on Pattern Analysis and Machine Intelligence*, vol. 22, no. 11, pp. 1330–1334, Nov. 2000. doi: 10.1109/34.888718

[38] Y. Hanaoka, I. Suzuki, and T. Sakurai, "Practical method to derive nonlinear response functions of cameras for scientific imaging," *Applied Optics*, vol. 50, no. 16, pp. 2401–2407, Jun. 2011. doi: 10.1364/AO.50.002401

[39] R. Pu, *Hyperspectral Remote Sensing: Fundamentals and Practices*, pp. 1–466, Jan. 2017. doi: 10.1201/9781315120607

[40] H. Akima, "A method of bivariate interpolation and smooth surface fitting based on local procedures," *Communications of the ACM*, vol. 17, no. 1, pp. 18–20, Jan. 1974. doi: 10.1145/360767.360779

[41] G. A. Blackburn, "Relationships between spectral reflectance and pigment concentrations in stacks of deciduous broadleaves," *Remote Sensing of Environment*, vol. 70, no. 2, pp. 224–237, Nov. 1999. doi: 10.1016/S0034-4257(99)00048-6

[42] C. Wu, Z. Niu, Q. Tang, and W. Huang, "Estimating chlorophyll content from hyperspectral vegetation indices: Modeling and validation," *Agricultural and Forest Meteorology*, vol. 148, no. 8–9, pp. 1230–1241, Jul. 2008. doi: 10.1016/j.agrformet.2008.03.005

[43] A. Zolotukhina *et al.*, "Evaluation of leaf chlorophyll content from acousto-optic hyperspectral data: A multi-crop study," *Remote Sensing*, vol. 16, no. 6, 1073, Mar. 2024. doi: 10.3390/rs16061073

[44] Z. Ye *et al.*, "A hyperspectral deep learning attention model for predicting lettuce chlorophyll content," *Plant Methods*, vol. 20, no. 1, pp. 1–11, Dec. 2024. doi: 10.1186/s13007-024-01148-9

[45] J. Zu *et al.*, "Inversion of winter wheat leaf area index from UAV multispectral images: Classical vs. deep learning approaches," *Frontiers in Plant Science*, vol. 15, 1367828, Mar. 2024. doi: 10.3389/fpls.2024.1367828

[46] B. Mandrapa *et al.*, "Machine learning-based hyperspectral wavelength selection and classification of spider mite-infested cucumber leaves," *Experimental and Applied Acarology*, vol. 93, no. 3, pp. 627–644, Oct. 2024. doi: 10.1007/s10493-024-00953-0

[47] L. J. S. Jong *et al.*, "Separating surface reflectance from volume reflectance in medical hyperspectral imaging," *Diagnostics*, vol. 14, no. 16, Aug. 2024. doi: 10.3390/diagnostics14161812

[48] M. S. Chiu and J. Wang, "Evaluation of machine learning regression techniques for estimating winter wheat biomass using biophysical, biochemical, and UAV multispectral data," *Drones*, vol. 8, no. 7, 287, Jun. 2024. doi: 10.3390/drones8070287

[49] L. Daniels, E. Eeckhout *et al.*, "Identifying the optimal radiometric calibration method for UAV-based multispectral imaging," *Remote Sensing*, vol. 15, no. 11, 2909, Jun. 2023. doi: 10.3390/rs15112909

[50] S. K. Vishwakarma *et al.*, "Mapping crop water productivity of rice across diverse irrigation and fertilizer rates using field experiment and UAV-based multispectral data," *Remote Sensing Applications: Society and Environment*, vol. 37, 101456, Jan. 2025. doi: 10.1016/j.rsase.2025.101456

[51] A. A. Gitelson, Y. J. Kaufman, and M. N. Merzlyak, "Use of a green channel in remote sensing of global vegetation from EOS-MODIS," *Remote Sensing of Environment*, vol. 58, no. 3, pp. 289–298, Dec. 1996. doi: 10.1016/S0034-4257(96)00072-7

[52] A. R. Huete, R. D. Jackson, and D. F. Post, "Spectral response of a plant canopy with different soil backgrounds," *Remote Sensing of Environment*, vol. 17, no. 1, pp. 37–53, Feb. 1985. doi: 10.1016/0034-4257(85)90111-7

[53] J. E. Gallagher and E. J. Oughton, "Surveying You Only Look Once (YOLO) multispectral object detection advancements, applications, and challenges," *IEEE Access*, vol. 13, pp. 7366–7395, 2025. doi: 10.1109/ACCESS.2025.3526458

[54] L. Smeesters, F. Venturini, S. Paulus *et al.*, "2025 photonics for agrifood roadmap: Towards a sustainable and healthier planet," *Journal of Physics: Photonics*, vol. 7, no. 3, 032501, Jun. 2025. doi: 10.1088/2515-7647/adbea9